Supporting Information for

Multifunctional Protein Nanowire Humidity Sensors for Green Wearable Electronics

Xiaomeng Liu, Tianda Fu, Joy Ward, Hongyan Gao, Bing Yin, Trevor Woodard, Derek R. Lovley, Jun Yao

---

This PDF file includes:

Materials and Methods

Synthesis and purification of protein nanowires.

Geobacter sulfurreducens was routinely cultured at 25 ℃ under strict anaerobic conditions (80/20 N_2-CO_2) in chemostats[1] in the previously described[2] mineral based medium containing acetate (15 mM) as the electron donor and fumarate (40 mM) as the electron acceptor. Cells were collected with centrifugation and re-suspended in 150 mM ethanolamine buffer (pH 10.5). The protein nanowires were harvested and purified as previously described.[3] These preparations yield protein nanowires with diameters of 3 nm,[4] consistent with being assembled from the pilin monomer PilA.[5] Briefly, protein nanowires were sheared from the cells in a blender. Cells were removed with centrifugation. The protein nanowires in the supernatant were precipitated with ammonium sulfate followed by centrifugation. The precipitate was re-suspended in ethanolamine buffer and additional debris was removed with centrifugation. The protein nanowires were collected with a second 10% ammonium sulfate precipitation and subsequent centrifugation at 13,000 g. The protein nanowires were re-suspended in ethanolamine buffer. This protein-nanowire preparation was dialyzed against deionized water to remove the buffer and stored at 4 °C. The resultant nanowire preparation yielded a measured pH~7.

Device fabrications.

The fabrication process of protein nanowire sensor was as follows (Figure S1). (1) A thin layer of polyimide (PI-2545; HD Microsystems) was spin coated (3000 rpm) on a Si wafer (3 inch P(100) 0-100 Ω·cm; UniversityWafer Inc.), followed by soft baking at 150 ℃ for 5 min and curing at 250 ℃ in an oven for 2 hr. Interdigitated electrodes were defined on PI film through standard photolithography, metal evaporation (Au/Cr = 30/5 nm) and lift-off processes. The 20 interdigitated electrodes in each device typically had a width ~300 μm, length ~0.5 cm, and intra-electrode separation ~100 μm. (2) The PI film with interdigitated electrodes was released from the Si substrate by using an electrochemical etching-assisted delamination method reported previously.[6] (3) The released PI layer, with defined electrodes, was floating on a water surface. (4) A pick-up substrate was then prepared as follows. First, a thin layer of polymethyl methacrylate (PMMA, 950 C2; MicroChem) was spin coated (1000 rpm, 60 s) on a glass slide and baked (100 ℃, 2 min). Then a layer of polydimethylsiloxane (PDMS, Sylgard 184, 10:1 mix ratio; Dow Corning) was spin coated (1000 rpm, 60 s) on the PMMA layer, yielding an estimated ~80 μm thickness.[7] The PDMS layer was curled at 90 ℃ for 1 hr. The PI film floating on the water was picked up by the glass slide coated with PDMS/PMMA layers. (5) Protein nanowire solution (~100 μl) was drop casted on the interdigitated electrode area, which was then placed on a hotplate (~80 ℃) to facilitate solvent (water) evaporation to form protein nanowire film. (6) A patch area containing the nanowire device was carved out, and the patch was then released from the glass substrate by using acetone droplet

to dissolve the PMMA layer. The electrodes in the device were wired using silver paste for electrical characterizations.

Humidity control.

The relative humidity (RH) was controlled through two approaches. First, carrier gases (*e.g.*, N_2, O_2, air) bubbling through a water-containing conical flask was led into a gas-purge desiccator cabinet (H42053-0002; Bel-91 Art), and the flow rate was adjusted to control the RH in the desiccator cabinet. The RH was real-time monitored by a hygrometer (Model 8706; REED Instruments). The bubbler method was used for controlled RH in measurements of moisture adsorption and device response time. Alternatively, RH was controlled by tuning the equilibrium vapor pressure of sulfuric acid solutions,[8] *i.e.*, the concentration of sulfuric acid (for FTIR measurements).

Device and material characterizations.

The thicknesses in protein nanowire films were measured by a desktop scanning electron microscope (SEM, EM-30 Plus; Element Pi). The high-resolution nanowire networks were imaged by using a transmission electron microscope (TEM, JEM-2200FS; JEOL). The H_2O bonding spectra in protein nanowires were performed by a Fourier-transform infrared spectroscopy (FTIR; Perkin Elmer) equipped with a universal attenuated-total-reflection (ATR) sampling accessory. *I-V* and *I-t* curves were measured by using a source meter (Keithley 2401; Tektronix) interfaced with computerized recording software or a current amplifier (1211 current preamplifier; DL Instruments) connected to A/D converter (Digidata 1440A; Molecular Devices) interfaced with a computer running recording software.

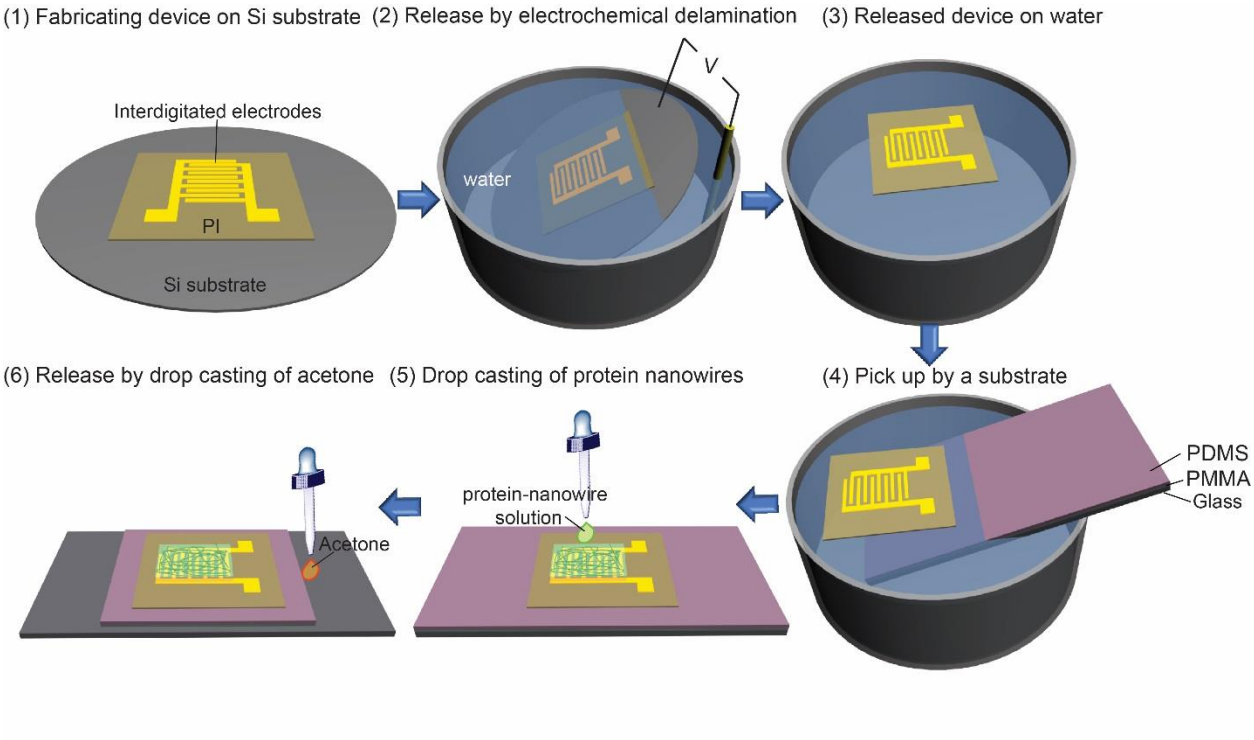

Figure S1. Schematics of the device fabrication process. The detailed description of each step can be found in the *Materials and Methods* section.

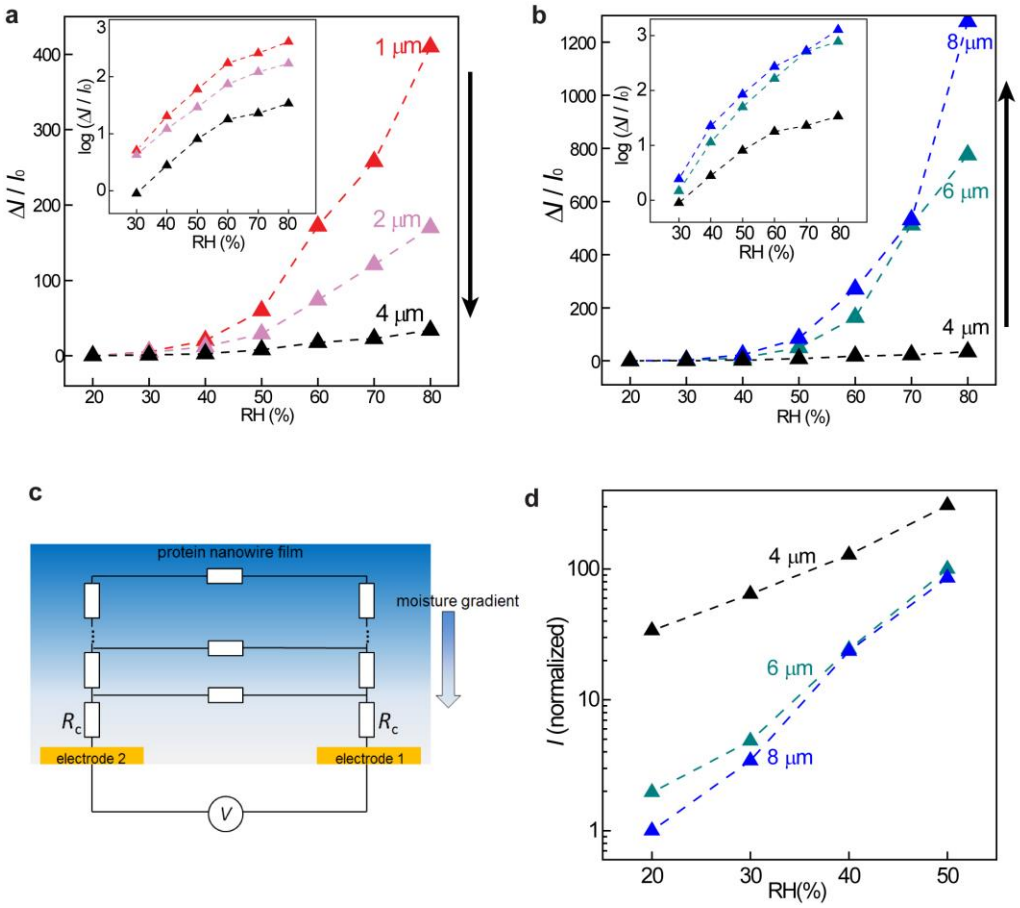

Figure S2. Film-thickness dependence in sensor response. (**a**) Relative current change ($\Delta I/I_o$) (I_o measured at a baseline RH of 20%) in protein nanowire sensors with film thickness of 1 μm (red), 2 μm (purple), and 4 μm (black), respectively. Inset shows the logarithmic plot. A decrease in sensor response was observed with the increase in nanowire film thickness. (**b**) $\Delta I/I_o$ in protein nanowire sensors with film thickness of 4 μm (black), 6 μm (cyan), and 8 μm (blue), respectively. Inset shows the logarithmic plot. An increase in sensor response was observed with the increase in nanowire film thickness.

(**c**) Cross-section schematics of a protein nanowire device and the equivalent circuit. The opposite trend in thick film can be understood from the existence of a vertical moisture gradient in the protein nanowire film.[3] The bottom interface was revealed to have reducing moisture adsorption with increasing film thickness, due to the unique chemical and structural properties in protein nanowires.[3] For a thick film, this means that overall sensor resistance is dominated by a high contact resistance (R_C) contributed from a layer of moisture-depletion nanowires at the bottom electrodes. (**d**) The analysis in (c) was supported by the observation that the overall device conduction decreased with the increase in film thickness at low RH≤ 50%.

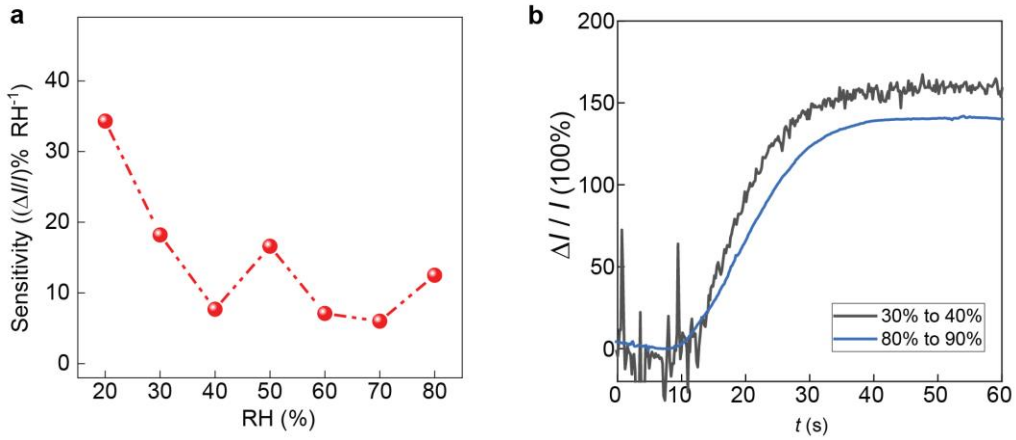

Figure S3. Sensor sensitivity at different relative humidity (RH). (**a**) Extrapolated (from Fig. 2a) sensor sensitivity, defined as the percentage change in conductance per percentage change in RH ($(\Delta I/I)\%\ RH^{-1}$), at different RH baselines. The protein nanowire sensor maintained a sensitivity > 6% RH^{-1}. (**b**) Real-time sensor responses to a 10% RH change at the baseline RH of 30% (gray) and 80% (blue), respectively. The sensor showed similar response at the low and high RH baselines, consistent with extrapolated sensitivity in (a).

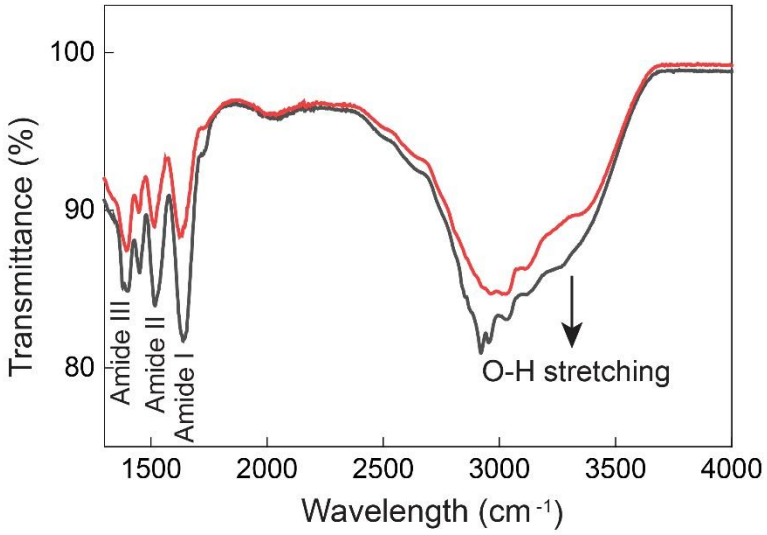

Figure S4. FTIR spectra of protein nanowire films at relative humidity (RH) of 20% (red curve) and 40% (gray curve). The broad peak ~3400 cm^{-1} corresponds to the O-H stretching band in free water,[9] and the increased intensity (gray curve) indicates increased water adsorption in the film at higher relative humidity. The increased intensities in other peaks could be caused by protein segments that became more mobile after moisture filling interstitial voids.

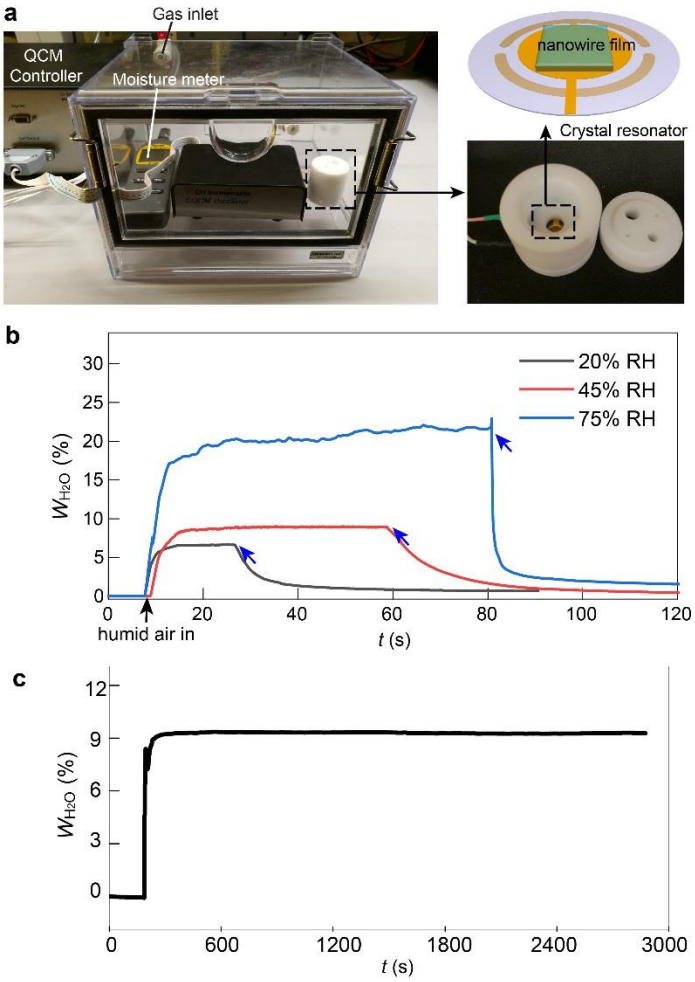

Figure S5. Moisture-adsorption measurement in thin films. (**a**) The measurement setup. It includes a gas-purge desiccator cabinet (H42053-0002; Bel-Art) with an inlet and outlet that allow the controlled flow of dry air, a portable hygrometer (Model 8706; REED Instruments) that can real-time monitor the relative humidity (RH) in the cabinet, and a quartz crystal microbalance (QCM; 400C, CH Instruments) that can monitor the thin-film mass. The protein nanowire film was first deposited on the quartz crystal resonator (right top) by drop casting. The mass sensitivity of the QCM originates from the dependence of the oscillation frequency on the total mass of the metal-coated crystal, including any deposited material. The mass change can be determined by $\Delta m = -\Delta f \cdot A \cdot \frac{\sqrt{\mu\rho}}{2f_0^2}$, where f_0, A, ρ, μ are resonant frequency of crystal's fundamental mode, area of the gold disk on the crystal, crystal's density (2.684 g cm^{-3}) and shear modulus of quartz (2.947×10^{11} g cm^{-1} s^{-2}), respectively.[10] We first determined the mass of the dry film (W_{film}) in a RH~0% environment by constant dry air flow. Then the flow was switched to bubbling air to increase the RH in the desiccator cabinet. During the process, the mass change (ΔW_{film}) that corresponds to the amount of moisture adsorption in the film, was continuously monitored (reflected by the resonant-frequency change in QCM). The moisture weight percentage $W_{H_2O}\%$ in the film was determined by: $W_{H_2O}\% = \Delta W_{film}/W_{\text{film}}\times100\%$. (**b**) Measured moisture content $W_{H_2O}\%$ in a protein nanowire film (~2 μm) at RH of 20%, 45% and 75%. A trend of increased moisture adsorption with increased RH was observed. The black and blue arrows indicating the start of flowing bubbling air and dry air, respectively. (**c**) The adsorbed moisture was measured to be stable in the protein nanowire film at fixed RH (~40%).

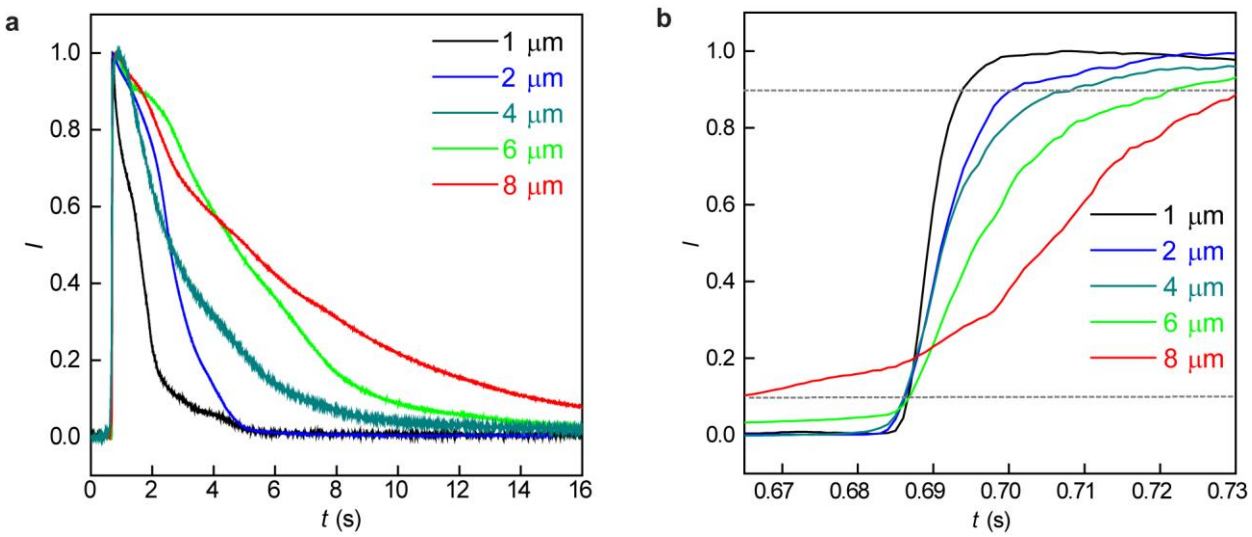

Figure S6. Thickness-dependent sensor response. (**a**) The sensor response to an instant increase of RH from 30% to 90% and instant removal. The decay times, defined as the time for the signal to reduce to 10% of the peak value, were 2.1 s, 2.9 s, 7.4 s, 12.4 s, and 15.3 s for nanowire film thickness of 1 μm, 2 μm, 4 μm, 6 μm, and 8 μm, respectively. (**b**) The response times, defined as the rising time from a 10% to 90% signal change (dashed lines), were 7 ms, 14 ms, 23 ms, 37 ms, and 69 ms for nanowire film thickness of 1 μm, 2 μm, 4 μm, 6 μm, and 8 μm, respectively.

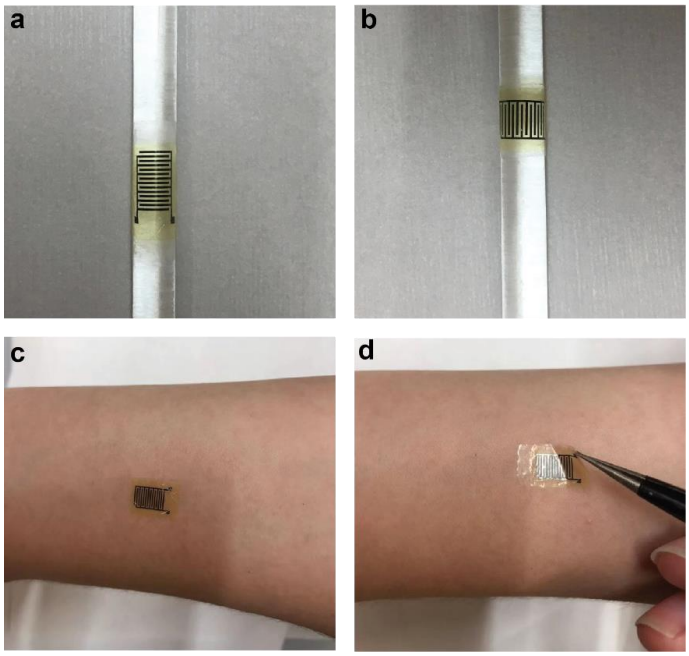

Figure S7. Conformal interfaces. Fabricated device on a flexible PDMS patch (see process in Figure S1) can conformally cover (**a**, **b**) surface curvature (diameter ~5 mm) of a glass rod and (**c**, **d**) human skin.

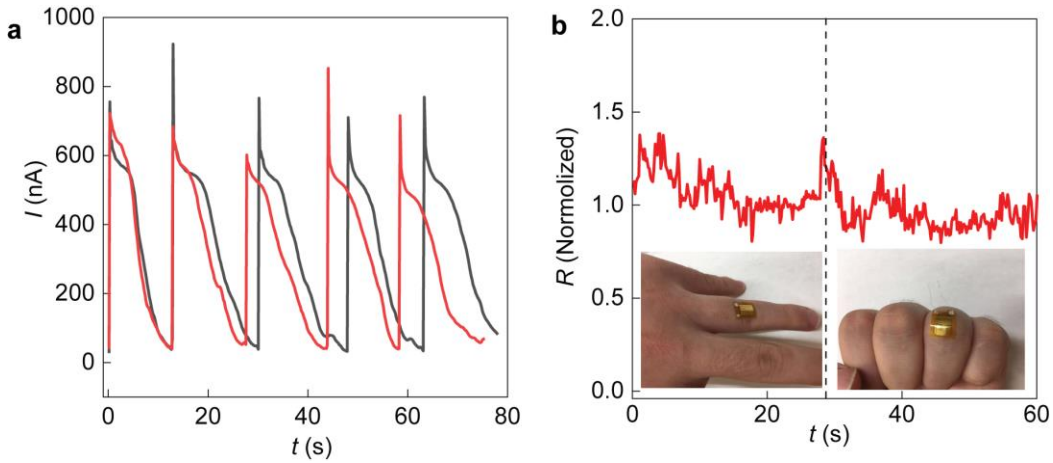

Figure S8. Mechanical testing. (**a**) The sensor response with respect to the repeated change of relative humidity (RH) between 45% and 92% in flat (black) and bending (red) state (with the bending radius of 0.5 mm). (**b**) Continuous monitoring of the (normalized) resistance in a protein nanowire sensor attached to a finger joint, before (left) and after (right) finger bending. The signal fluctuations largely came from local RH variations during the movements.

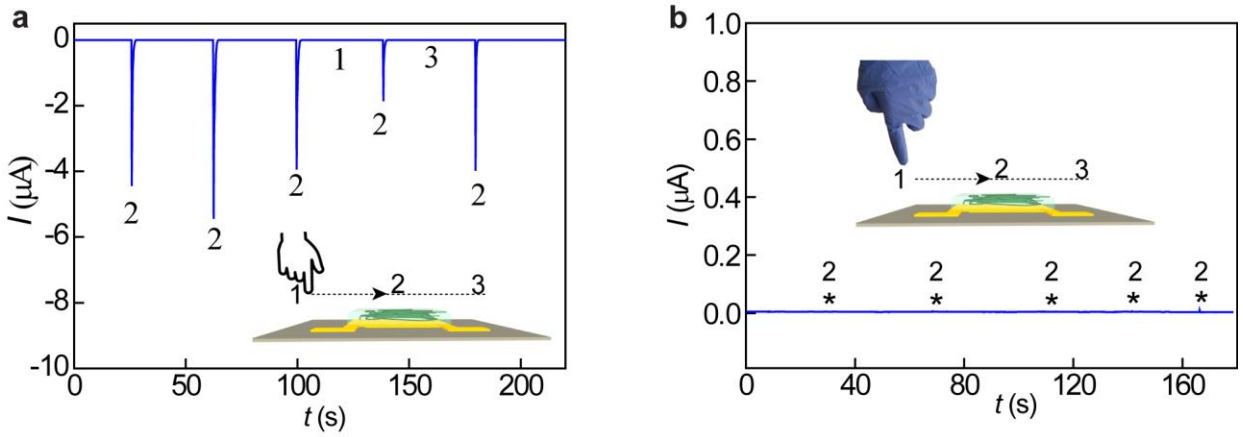

Figure S9. Sensor responses from moving fingers. (**a**) Current responses from a protein nanowire device to repeated (5 times) finger movements of swiping across. The bias voltage was flipped (V_{bias} = -1 V) from that in Fig. 3d. The inset shows the schematic of the finger track, with the numbers indicating the positions. (**b**) Current responses from a protein nanowire device to repeated (5 times) finger movements of swiping across, with the finger wearing a glove.

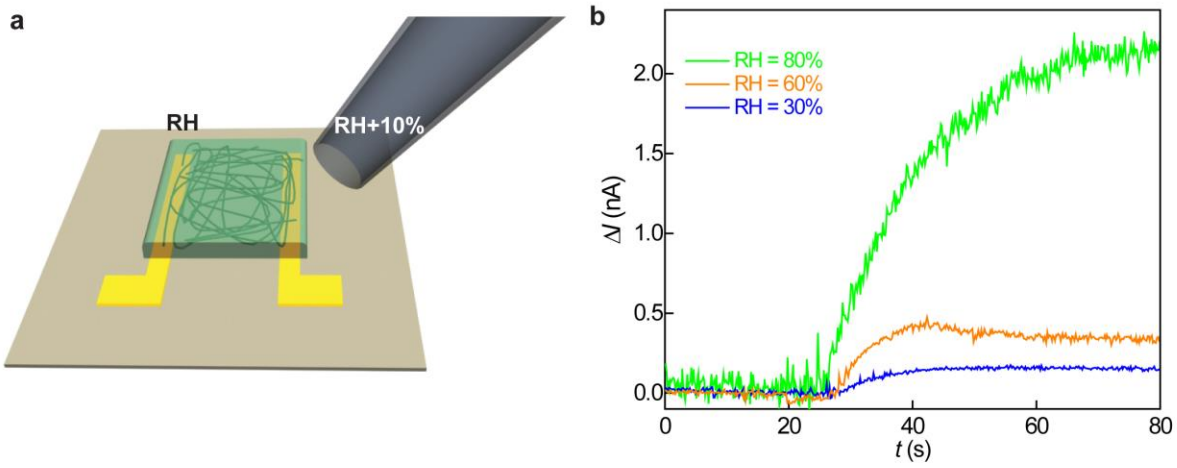

Figure S10. Humidity-dependent powerless sensing. (**a**) Schematic of the experimental setup to control the humidity difference between the two electrodes. The protein nanowire device was first exposed to a stable relative humidity (RH) background. Air of higher RH (*e.g.*, ΔRH = 10%) was then blew from one side to increase the local RH at one electrode. During the process, the current output (Δ*I*) from the device was monitored, with no external voltage applied. Both the background and flowing RHs were controlled by equilibrium vapor pressure of sulfuric acid solutions.[5] (**b**) Generated current (Δ*I*) at different background RH of 30%, 60%, and 80%. A trend of increasing current signal was observed with the increase in background RH.

This RH-dependent signal can be generally understood. The signal is $\Delta I = V_o/R$, where V_o is a generated open-circuit voltage. Our previous study showed that the voltage output (V_o) was approximately proportional to the difference of moisture adsorption between the two electrodes.[6] Since the moisture adsorption is roughly proportional to RH (Fig. S5b), it indicates that for fixed ΔRH, V_o should stay relatively close at different background RH. To the contrary, *R* is highly sensitive to RH and hence expected to play the determining role in Δ*I*. Since *R* decreases substantially with increasing RH (Fig. 2a), Δ*I* is expected to increase with increasing background RH as observed.

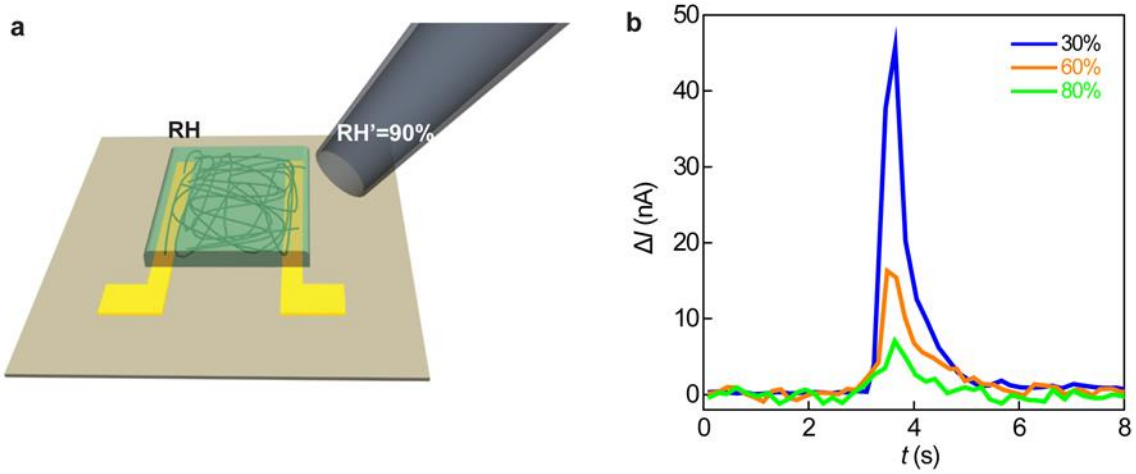

Figure S11. Humidity-dependent powerless sensing. (**a**) For practical wearable application (*e.g.*, breathing detection), usually the peak of the instant RH' is fixed independent of the background/ambient RH. We experimentally emulated breathing by flowing air (RH'~90%) from one side of the device to create instant humidity gradient. (**b**) Generated current (ΔI) at different background RH of 30%, 60%, and 80%. A trend of decreasing current signal was observed with the increase in background RH.

We can do similar analysis to understand the trend. The signal is $\Delta I = V_o/R$, where V_o is a generated open-circuit voltage. Since R is determined by the peak RH (hence fixed), it is expected that the generated current signal I_t will be largely dependent on V_{out}. Previous study showed that the voltage output (V_o) was approximately proportional to the difference of moisture adsorption between the two electrodes.[3] Since the moisture adsorption is roughly proportional to RH (Fig. S5b), this means that V_{out} may be roughly proportional to ΔRH (*e.g.*, 90%-RH). Therefore, a lower background RH will then lead to higher ΔRH and higher I_t as shown in (b).

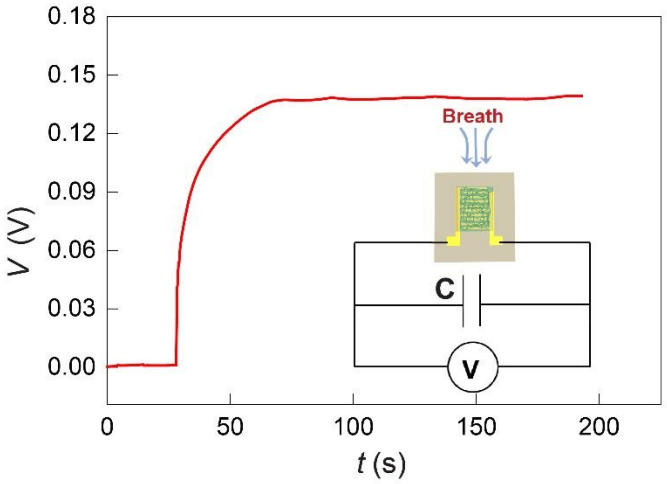

Figure S12. Electric power generation. Instant humidity gradient in percolative conductive films was shown to yield electric potential gradient and hence a measured voltage output.[11] Here we demonstrated that the protein nanowire device could generate a ~0.13 V output voltage by a humidity gradient induced by a breath, which could be used to charge up a capacitor (10 μF). Note that because the protein nanowire device had a substantially increased resistance at lower RH (Fig. 2a), the discharging time (RH reduced after breath) was much slower than the charging time using the circuit shown in the inset.

References

1. A. Esteve-Núñez, M. M. Rothermich, M. Sharma, D. R. Lovley, *Environ. Microbiol*. **2005**, *7*, 641-648.
2. M. V. Coppi, C. Leang, S. J. Sandler, D. R. Lovley, *Appl. Environ. Microbiol*. **2001**, *67*, 3180-3187.
3. X. Liu, H. Gao, J. Ward, X. Liu, B. Yin, T. Fu, J. Chen, D. R. Lovley, J. Yao, *Nature* **2020**, 578, 550.
4. T. Fu, X. Liu, H. Gao, J. E. Ward, X. Liu, B. Yin, Z. Wang, Y. Zhuo, D. J. F. Walker, J. J. Yang, J. Chen, D. R. Lovley, J. Yao, *Nat. Commun*. **2020**, 11, 1861.
5. D. R. Lovely, D. Walker, *Front. Microbiol.* **2019**, 10, 2078.
6. H. Zhang, Y. Liu, C. Yang, L. Xiang, Y. Hu, L.-M. Peng, *Adv. Mater*. **2018**, *30*, 1805408.
7. W. Y. Zhang, G. S. Ferguson, S. Tatic-Lucic, *Proc. 17th IEEE Intern. Conf. on Micro Electro Mechanical Systems* **2004**, pp. 741-744.
8. J. Feng, L. Peng, C. Wu, X. Sun, S. Hu, C. Lin, J. Dai, J. Yang, Y. Xie, *Adv. Mater*. **2012**, *24*, 1969-1974.
9. J. Kong, S. Yu, *Acta. Biochim. Biophys. Sin*. **2007**, *39*, 549-559.
10. http://www.chinstruments.com/chi400.shtml.
11. F. Zhao, H. Cheng, Z. Zhang, L. Jiang, L. Qu, *Adv. Mater*. **2015**, *27*, 4351-4357.